Volume 8, Issue 3, 2018, 3282 - 3288 **ISSN 2069-5837**

Biointerface Research in Applied Chemistry

www.BiointerfaceResearch.com

Original Research Article **Open Access Journal**

Received: 06.05.2018 / Revised: 10.06.2018 / Accepted: 12.06.2018 / Published on-line: 15.06.2018

Application of quantum chemical calculations in modeling of the supramolecular nanomedicine constructed from host-guest complexes of cucurbit[7]uril with gemcitabine anticancer drug

Rezvan Mohammadabadi [1], Ali Morsali [1, 2, *], Mohammad M. Heravi [1], S. Ali Beyramabadi [1, 2]

[1] Department of Chemistry, Mashhad Branch, Islamic Azad University, Mashhad, Iran
[2] Research Center for Animal Development Applied Biology, Mashhad Branch, Islamic Azad University, Mashhad 917568, Iran
*corresponding author e-mail address***: *almorsali@yahoo.com***

ABSTRACT

Using a quantum mechanical approach, we have investigated the drug delivery efficiency of cucurbit[7]uril for gemcitabine anticancer drug in gas and solution phases. The eight noncovalent interactions of drug gemcitabine with cucurbit[7]uril have been considered and optimized at M06-2X/6-31G(d,p) level. The calculation of binding energies showed the energetic stability of the host-guest complexes and confirmed the physical nature of interactions. It was specified that the gas phase binding energies are more negative than those of solution phase. The host-guest complex in which the drug is encapsulated in cucurbit[7]uril, is the most stable configuration and has the major contribution in gemcitabine drug delivery. Also, the free energies of solvation and quantum molecular descriptors were calculated. The free energies of solvation show that gemcitabine solubility increases in the vicinity of cucurbit[7]uril. The values of gemcitabine quantum molecular descriptors such as global hardness and HOMO-LUMO energy gap are higher than those of cucurbit[7]uril, showing the reactivity of the gemcitabine increases. The AIM analysis demonstrated that the hydrogen bonding between OH and NH_2 functional groups of gemcitabine and the carbonyl functional group of cucurbit[7]uril plays an important role in the gemcitabine drug delivery.

Keywords: *Cucurbit[7]uril; Quantum molecular descriptors; Gemcitabine; Host-guest complexes; AIM analysis; Density functional theory.*

1. INTRODUCTION

Since the decline of traditional medicine and the introduction of modern pharmacology, there has always been the challenging issue of the effectiveness of the modern drugs in connection with their stability and uniqueness of action. The researchers found that a possible solution to this challenging problem could produce structures that could carry a therapeutic agent and release it within a specified time and at a given site. Consequently, efforts have been made recently with the objective of producing controlled and targeted drug delivery carriers [1-3].

To materialize the above mentioned objective, a technique involving the encapsulation of the drug by a macrocyclic host was used, which safeguarded the drugs from degradation by utilizing steric hindrance. The objectives of the encapsulation of therapeutic agents are the rise of drug solubility, modification of the drug delivery and its maintaining in the body, alteration of the mechanism of drug penetration, control the drug release, reducing the level of an agent's degradation and improvement in the stability of shelf life [4-7].

These techniques, known as host-guest method, have been extensively used in medicinal and biological applications. Examples of such applications are pharmaceutical synthesis [8,9], drug delivery [10,11], detections of biological analysts [12-14], agricultural fields [15] and diagnostic tools [16]. A number of measures and conditions must be fulfilled before the application of host molecules as carriers in pharmaceutical compounds. The most vital conditions to be satisfied for these molecules are their biological inertness, nontoxicity, and chemical stability, which enable them to create complexes having a high degree of binding to medicinal compounds and making them controllable [17].

Dendrimers [18] are defined to be highly branched macromolecules and normally regarded as polymers, for the reason that their structure could be defined by many repeated subunits [19]. Most of the molecular identification work carried out with dendrimers have been performed by using cucurbit[n]urils and cyclodextrins as host particles [20]. Lately, cucurbit[n]urils (CB[n]) has demonstrated utility as drug delivery carriers [10,21,22].

Behrend synthesized cucurbiturils in 1905 through condensing glycoluril and formaldehyde in an acidic environment. Freeman described the chemical structure of cucurbiturils in 1981 [16]. Till 2000, CB[6] was the only CB[n] to catch any consideration as a molecule beneficial in host–guest complexes. This altered upon the finding of diverse sized cucurbit[n]urils: CB[5] to CB[10] [21,22]. Their discovery has resulted in a rapid rise in the application of CB[n] in various areas involving drug delivery and molecular machines [23].

Cucurbit[n]urils are comparatively water-soluble particles that have a rather inflexible, definite cavity whose inside surface is characterized as hydrophobic, being capable of creating complexes with various guests in aqueous solution [24,25]. CB[n] (n = 5, 6, 7, 8, 10) homologues have 5-10 glycoluril residues which make hydrophilic surface (carbonyl functional groups). Binding of cucurbiturils with molecules could take place by hydrophobic interactions inside the cavity, ion–dipole interactions and the formation of hydrogen bonds between the oxygen at the

hydrophilic surface of the host and the hydrogen atoms of the guest [26-28].

Different molecules including anticancer compounds [29], DNA bases [30], amino acids [30], ranitidine [31], curcumin [32] and proflavine [33] have been encapsulated in CB[n]. The discovery of water soluble cucurbit[n]urils will increase the production of new and effective drug delivery carriers [23,34]. With the objective of increasing medicinal compounds stability and preventing the quick degradation of them, the therapeutic agents (particularly anticancer agents known for low stability in the body) are encapsulated into cucurbiturils [35,36]. Comparison between CB[5] to CB[8] shows that CB[7] is more soluble than CB[6] and CB[8] in aqueous solutions, as well as has a more capacious cavity than CB[5], and can consequently bind a wider range of molecules in water. Recently, the CB[7] was utilized to form complexes with some fluorescent dyes [37-40] to develop their photochemical stabilities and fluorescence yields in aqueous solutions [41]. In addition, cucurbit[n]urils have advantages such high drug loading capacities and low toxicity which make them appropriate candidates for being used in drug delivery [42-44].

Presentation of proper molecular models in aqueous solutions is of special importance in understanding the mechanistic behavior of drug delivery systems [45-50]. The most suitable method for presenting such molecular models is quantum mechanical calculations. The 2016 chemistry Nobel Prize was awarded to the design of molecular machines, an important application of which is in the drug delivery systems [51-53].

In this work, noncovalent interactions of cucurbit[7]urils with gemcitabine drug have been analyzed using quantum mechanical calculations. Gemcitabine or 4-amino-1-[(2R,4R,5R)-3,3-difluoro-4-hydroxy-5-(hydroxymethyl)oxolan-2-yl]pyrimidin-2-one has antitumor, antiviral and anticancer activities and is highly effective in the treatment of pancreatic, head, neck, breast and non-small cell lung cancers [54,55]. This work could inspire the researchers to design and manufacture of new drug delivery systems.

2. EXPERIMENTAL SECTION

Computational details. We performed full geometry optimizations for all CB[7]-gemcitabine configurations in aqueous solution at the M06-2X/6-31G(d,p) level, using Gaussian 2009 package [56]. The solvent has an important role in different biological and chemical systems explicitly [57-61] or implicitly. Polarized continuum model (PCM) [62,63] was utilized for implicit effects of the solvent. SMD solvation model [64] was used for the evaluation of solvation energies. In SMD model, the free energy of solvation is evaluated using the following equation:

$$\Delta G_{Solv} = (\Delta G_{Solv} + \Delta G_{nonelectrostatic}) - E_{gas} \quad (1)$$

where E_{solv} and E_{gas} show the total energies of the system in the solution phase and gas phase, respectively, and $\Delta G_{nonelectrostatic}$ is the nonelectrostatic energy.

The AIM computations were performed using the AIMALL package [65]. QTAIM has been based on the topological analysis of the electron density, ρ(r) [66,67]. The topology of ρ(r) is under the impact of nuclear maxima, bond critical points (BCPs), indicating the lowest point of electron density between two nuclei and lines of maximum density (bond paths) linking the nuclear maxima of bonded nuclei. There are several properties of the electron density at a BCP for distinguishing the nature of the bond. These parameters include the electron density (ρ_b), the Laplacian of the electron density ($\nabla^2\rho$), the local electron kinetic (G_b), potential (V_b) and total (H_b) energy densities. The amount of both quantities ρ_b and $\nabla^2\rho$ is related to the strength of the bond between the two nuclei. In addition, the sign of $\nabla^2\rho$ together with the sign of the total energy density (H_b) at the BCP presents more information on the nature of the interactions. At the extreme ends of the scale, if $\nabla^2\rho > 0$ and $H_b > 0$ at the BCP, it shows that a closed shell interaction, while $\nabla^2\rho < 0$ and $H_b < 0$ indicates a covalence bond. The two other critical points, i.e., ring critical points (RCP) and cage critical points (CCP) show saddle points and local minima of the electron density, respectively.

3. RESULTS AND DISCUSSION

The optimized geometries of cucurbit[7]uril (CB[7]) and gemcitabine (Gem) anti-cancer drug in solution phase are presented in Figure 1. The interaction between CB[7] and Gem including configurations CB[7]/Gem1-CB[7]/Gem8 (host-guest complexes) was considered in gas and solution phases. These eight host-guest complexes have been shown in Figures 2 and 3.

The binding energies (ΔE) of Gem with CB[7] in gas and aqueous solution were calculated using equation (2) and represented in Table 1:

$$\Delta E = E_{\mathrm{CB[7]/Gem1-8}} - (E_{\mathrm{CB[7]}} + E_{Gem}) \quad (2)$$

All eight host-guest complexes represent different ΔEs depending on the orientation of Gem. The calculated binding energies of CB[7]/Gem1-8 are negative in both phases. ΔEs related to gas phase are more negative than those related to solution phase (Table 1). CB[7]/Gem1 is the most stable configuration in both phases. This is mainly because of the orientation of Gem with respect to CB[7]. In this configuration, Gem has been encapsulated in CB[7].

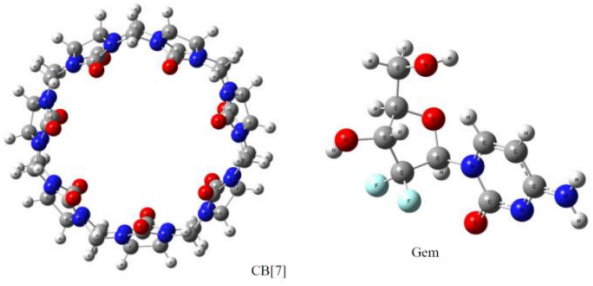

Figure 1. Optimized structures of CB[7] and Gem.

Table 1. Solvation and binding energies of Gem, CB[7] and CB[7]/Gem1-8 in gas and solution phases (kJ/mol).

Species	Solvation energy	Binding energy	Binding energy
		Solution phase (pcm)	Gas phase
Gem	-110.95		
CB[7]	-557.29		
CB[7]/Gem1	-603.34	-123.75	-188.89
CB[7]/Gem2	-644.46	-88.075	-106.56
CB[7]/Gem3	-655.44	-107.32	-116.86
CB[7]/Gem4	-602.75	-66.86	-129.67
CB[7]/Gem5	-646.05	-56.86	-89.61
CB[7]/Gem6	-629.51	-65.07	-104.34
CB[7]/Gem7	-634.42	-97.05	-110.34
CB[7]/Gem8	-651.28	-105.70	-118.32

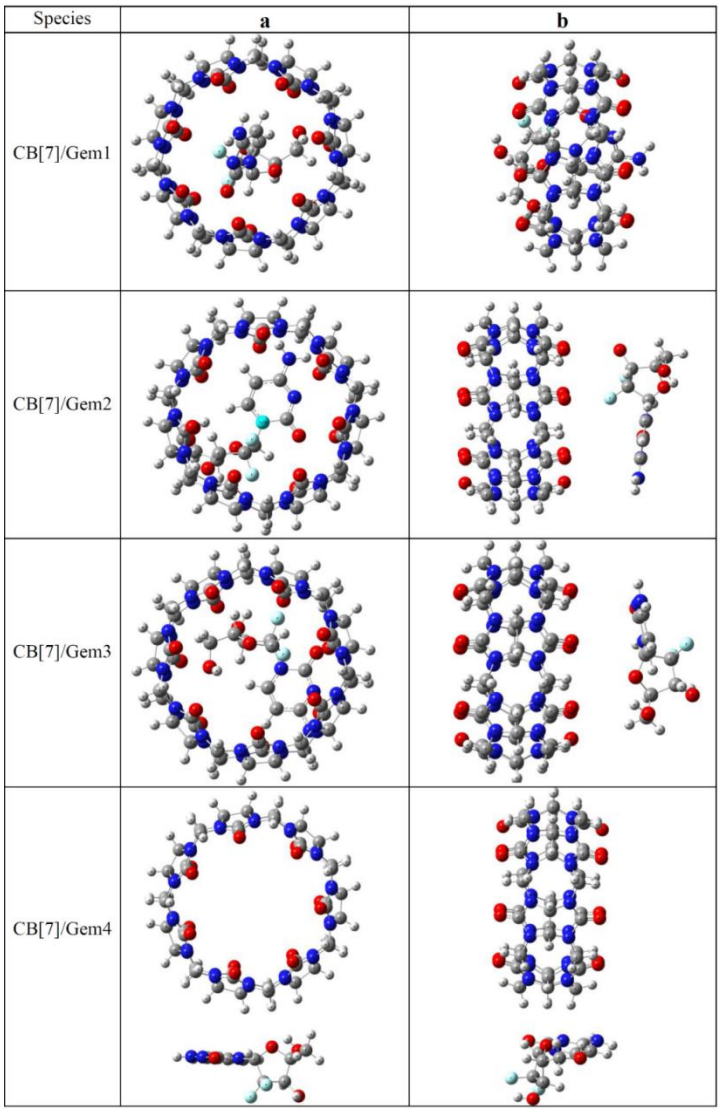

Figure 2. Optimized structures of CB[7]/Gem1-4 (a) bird's eye-view (b) side view.

The free energies of solvation (ΔG_{Solv}) have been evaluated using SMD model in aqueous solution. Water was selected for the evaluation of ΔG_{Solv}, because water can mimic the biological condition and is the most important solvent in the body. The negative values of ΔG_{Solv} indicate the degree of dissolution. The solvation energies of Gem, CB[7] and CB[7]/Gem1- CB[7]/Gem8 are shown in Table 1. The calculated ΔG_{Solv} show that Gem solubility increases in the presence of CB[7] and CB[7]/Gem3 has a higher solubility relative to other configurations. The important peculiarity of Gem drug is in having OH and NH_2 functional groups, causing strong hydrogen bond between the drug and CB[7] and this is the reason that makes this drug a proper candidate for delivery by CB[7]. Also, functionalization of CB[7] with Gem drug causes an increase in solubility of CB[7] which is an important factor for its applicability in the drug delivery. The enhanced solubility of all host-guest complexes demonstrates it to be appropriate for drug delivery and the noncovalent functionalization may have advantages in terms of dissolution and drug release over the covalent functionalization, where breakage of the covalent bond is accompanied with high barrier energy.

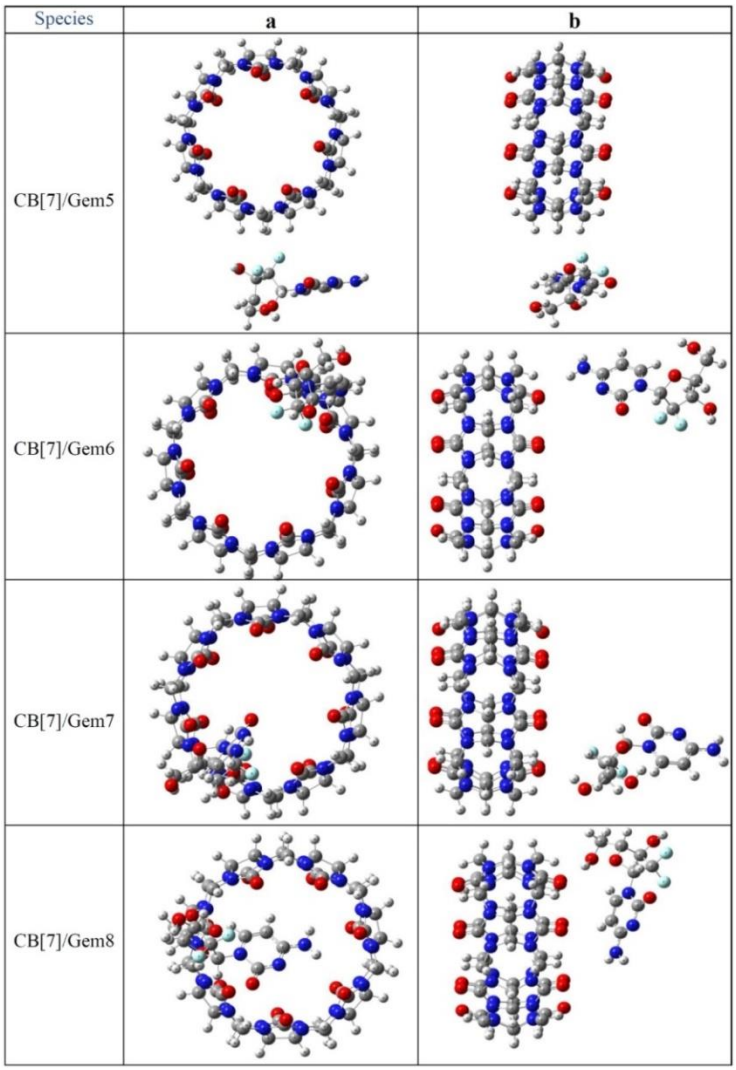

Figure 3. Optimized structures of CB[7]/Gem1-4 (a) bird's eye-view (b) side view.

We used quantum molecular descriptors including chemical potential, hardness, softness and electrophilicity index to characterize chemical reactivity and stability. The global hardness (η) describes the resistance against the change in molecular electronic structure (Equation (3)). η has a direct relation with the stability and inverse ratio with respect to the reactivity.

$$\eta = (I - A)/2 \qquad (3)$$

where $A = -E_{LUMO}$ and $I = -E_{HOMO}$ are the electron affinity and the ionization potential of the molecule, respectively. The electrophilicity index (ω) is formulated as follows [68]:

$$\omega = (I + A)^2/4\eta \qquad (4)$$

The chemical potential (μ) is defined by:

$$\mu = -(I + A)/2 \quad (5)$$

Softness (S) is inversely proportional to the η:

$$S = \frac{1}{\eta} \quad (6)$$

Table 2 lists the quantum molecular descriptors of Gem, CB[7] and CB[7]/Gem1-8, including the energy of the lowest unoccupied molecular orbital (E_{LUMO}), the energy of the highest occupied molecular orbital (E_{HOMO}), hardness (η), softness (S), the chemical potential (μ) and electrophilicity index (ω). In this table and Figure 4, Eg (gap of energy between LUMO and HOMO) determines a more stable configuration. Quantum calculations on Gem show it to be a stable species with high Eg values of 7.76 eV (gas phase) and 7.92 eV (solution phase) and high η values of 3.88 eV (gas phase) and 3.96 eV (solution phase). On the other side CB[7] is more stable than Gem with Eg values of 10.11 eV (gas phase) and 10.20 eV (solution phase). According to the values in Table 2, η and Eg related to the Gem drug are higher than those of CB[7]/Gem1-8 , showing the stability of Gem decreases in the presence of CB[7] and its reactivity increases. The ω values of CB[7] in gas (0.99 eV) and solution (1.07 eV) phases are lower than those of Gem (1.94 eV and 1.93 eV in gas and solution phases, respectively). In most cases, ω of Gem decreases in the presence of CB[7] , showing that Gem acts as electron donor.

HOMO and LUMO analysis is relatively useful in the specification of the charge localization and based on, charge distribution related to a molecule can be evaluated. The localization of electron density in HOMO makes the position to be nucleophilic. The HOMO and LUMO orbitals of CB[7]/Gem1, CB[7] and Gem have been shown in Figure 4 (solution phase).In the Gem structure, the HOMO is more localized on C-H bond in the six-membered ring and to a lesser extent on oxygen and nitrogen whereas LUMO is localized entirely on the ring. In complex CB [7] / Gem1, HOMO lies mainly on the Gem drug and no change is observed in its structure. Observations in the case of LUMO are the same. This distribution shows that physical adsorption of Gem through noncovalent interactions does not cause any important perturbation in the drug.

Theory of atoms in molecules is extensively used as a theoretical instrument for the analysis and understanding of chemical bonds. This theory has been made on the basis of the critical points (CPs) of the molecular electronic charge density ρ(r). Generally, ρ(r) is more than 0.20 a. u. and less than 0.10 a. u. in covalent bonding and closed-shell interaction, respectively. It has been shown that ρ(r) is severely correlated with the binding energy [55-60]. For strong interaction ($\nabla^2\rho < 0$ and $H_b < 0$), medium strength ($\nabla^2\rho > 0$ and $H_b < 0$) and weak interaction ($\nabla^2\rho > 0$ and $H_b > 0$), we have covalent bonding, partially covalent character and electrostatic, respectively [69]. For hydrogen bond, the values of ρ(r) and $\nabla^2\rho(r)$ are 0.002–0.035 a. u. and 0.024–0.139 a. u., respectively. The nature of intermolecular hydrogen bond could be characterized using $-G_b/V_b$, which for $-G_b/V_b > 1$, the noncovalent character is established, while for $0.5 < -G_b/V_b < 1$, it is partially covalent.

CB[7]/Gem1 and CB[7]/Gem3 are the most stable configurations in both phases. Now, we analyze the nature of the chemical bonds of these two structures in solution phase by using AIM. The molecular graphs including critical points and bond paths for CB[7]/Gem1 and CB[7]/Gem3 are shown in Figures 5 and 6, respectively. The values of the electron density (ρ(r)), its Laplacian ($\nabla^2\rho(r)$) , total energy density (H_b), electronic kinetic energy density (G_b), electronic potential energy density (V_b) and $-G_b/V_b$, at BCP, are given in Tables 3 and 4 for CB[7]/Gem1 and CB[7]/Gem3, respectively. In addition, using Espinosa method [70] the hydrogen bond energies ($E_{HB} = 1/2V_b$) have been calculated. According to Table 3, at the critical points (CP) 174 and 188, the O52 ⋯ H150 and O42 ⋯ H145 interactions in CB[7]/Gem1 ($\nabla^2\rho > 0$, $H_b < 0$ and $0.5 < -G_b/V_b < 1$) are classified as medium hydrogen bonds . Other interactions ($\nabla^2\rho > 0$, $H_b > 0$ and $-G_b/V_b > 1$) are related to the weak hydrogen bonds category. The values in Table 3 show that hydrogen bonding in the O52 ⋯H150 interaction is more stable than the bond in O42 ⋯H145. According to Table 4, the most stable interaction in CB[7]/Gem3 is O78 ⋯H145 interaction at CP 182, being of medium hydrogen bond and other interactions, being categorized as weak hydrogen bonds.

Table 2. Quantum molecular descriptors (eV) of Gem, CB[7] and CB[7]/Gem1-8.

Species	E_{HOMO}	E_{LUMO}	E_g	η	μ	ω	S
	Solution Phase (pcm)						
Gem	-7.87	0.05	7.92	3.96	-3.91	1.93	0.25
CB[7]	-8.40	1.79	10.20	5.10	-3.31	1.07	0.20
CB[7]/Gem1	-7.49	0.25	7.74	3.87	-3.62	1.69	0.26
CB[7]/Gem2	-7.77	0.03	7.81	3.90	-3.87	1.92	0.26
CB[7]/Gem3	-7.49	0.45	7.94	3.97	-3.52	1.56	0.25
CB[7]/Gem4	-8.03	-0.20	7.82	3.91	-4.12	2.17	0.26
CB[7]/Gem5	-7.99	-0.21	7.78	3.89	-4.10	2.16	0.26
CB[7]/Gem6	-7.76	0.13	7.90	3.95	-3.82	1.84	0.25
CB[7]/Gem7	-7.51	0.39	7.90	3.95	-3.56	1.60	0.25
CB[7]/Gem8	-7.39	0.56	7.95	3.98	-3.42	1.47	0.25
	Gas Phase						
Gem	-7.76	0.00	7.76	3.88	-3.88	1.94	0.26
CB[7]	-8.21	1.89	10.11	5.05	-3.16	0.99	0.20
CB[7]/Gem1	-6.44	1.34	7.78	3.89	-2.55	0.84	0.26
CB[7]/Gem2	-7.52	0.10	7.62	3.81	-3.71	1.81	0.26
CB[7]/Gem3	-5.86	1.55	7.41	3.70	-2.15	0.63	0.27
CB[7]/Gem4	-7.41	0.44	7.85	3.93	-3.48	1.54	0.25
CB[7]/Gem5	-7.94	-0.26	7.68	3.84	-4.10	2.19	0.26
CB[7]/Gem6	-7.35	0.51	7.86	3.93	-3.42	1.49	0.25
CB[7]/Gem7	-6.02	1.56	7.58	3.79	-2.23	0.66	0.26
CB[7]/Gem8	-5.94	1.56	7.50	3.75	-2.19	0.64	0.27

Table 3. Topological parameters in a. u. and the hydrogen bond energy (E_{HB}) in kJ/mol for CB[7]/Gem1 at m062x/6-31G(d,p).

BCP	Atoms	ρ(r)	∇^2_ρ(r)	G_b	V_b	H_b	$-G_b/V_b$	E_{HB}
34	N23⋯ H155	0.0105	0.0362	0.0082	-0.0072	0.0009	1.1242	-9.44
56	O36 ⋯ H152	0.0078	0.0284	0.0061	-0.0052	0.0010	1.1871	-6.82
136	N77 ⋯ H133	0.0053	0.0164	0.0035	-0.0029	0.0006	1.1970	-3.80
143	N79 ⋯ H133	0.0058	0.0182	0.0039	-0.0033	0.00061	1.1871	-4.33
164	O36 ⋯ H132	0.0104	0.0378	0.0084	-0.0073	0.0011	1.1447	-9.57
172	O44 ⋯ H149	0.0078	0.0286	0.0062	-0.0053	0.0009	1.1800	-6.95
174	O52 ⋯ H150	0.0241	0.0775	0.0196	-0.0198	-0.0002	0.9900	-25.97
178	O54 ⋯ N141	0.0080	0.0266	0.0063	-0.0059	0.0004	1.06531	-7.74
181	O14 ⋯ H139	0.0122	0.0370	0.0091	-0.0090	0.0001	1.0135	-11.80
184	O42 ⋯H139	0.0077	0.0292	0.0061	-0.0049	0.0012	1.2396	-6.43
188	O42 ⋯H145	0.0204	0.0670	0.0168	-0.0169	-9.1E-05	0.9946	-22.16
189	O54 ⋯H144	0.0119	0.0464	0.0104	-0.0092	0.0012	1.1297	-12.07
201	O13 ⋯H154	0.0076	0.0294	0.0063	-0.0052	0.0010	1.2021	-6.82
202	O22 ⋯ H152	0.0154	0.0518	0.0123	-0.0117	0.0006	1.0528	-15.34

Table 4. Same as Table 3 For CB[7]/Gem3.

BCP	Atoms	ρ(r)	∇^2_ρ(r)	G(r)	V(r)	H(r)	- G(r)/ V(r)	E_{HB}
92	H107 ⋯ O153	0.0094	0.0370	0.0078	-0.0064	0.0014	1.2201	-8.39
163	O66 ⋯ H137	0.0070	0.0289	0.0060	-0.0049	0.0012	1.2432	-6.43
165	O66 ⋯ H139	0.0078	0.0292	0.0062	-0.0052	0.0010	1.2013	-6.82
166	O78 ⋯ H139	0.0108	0.0369	0.0085	-0.0078	0.0007	1.0925	-10.23
180	O22 ⋯ H144	0.01416	0.0142	0.0115	-0.0115	5.6E-05	1.0049	-15.08
182	O78 ⋯ H145	0.0186	0.0591	0.0150	-0.0153	-0.0003	0.9819	-20.07

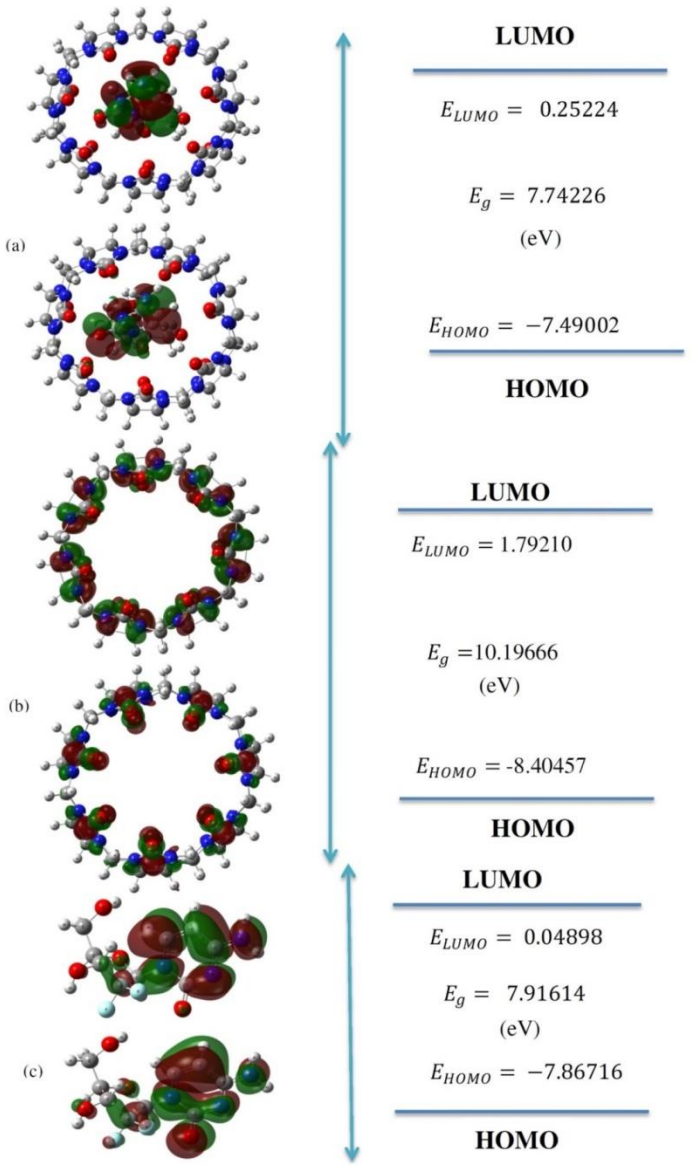

Figure 4.HOMO and LUMO for (a) CB[7]/Gem1 (b) CB[7] and (c) Gem.

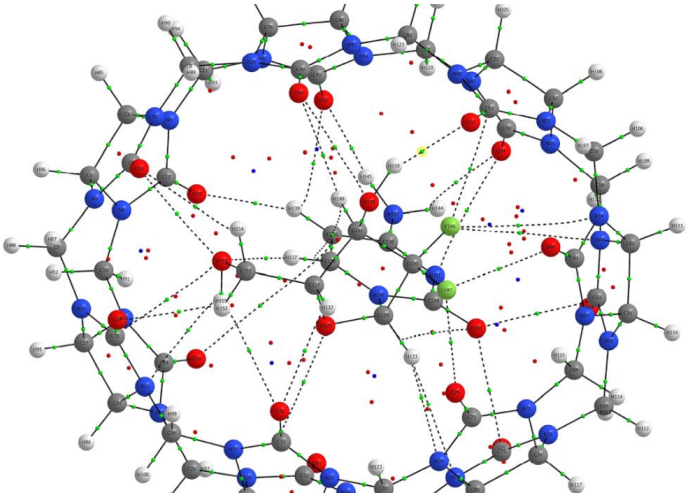

Figure 5. Molecular graph of CB[7]/Gem1. Small green spheres and lines correspond to the bond critical points (BCP) and the bond paths, respectively.

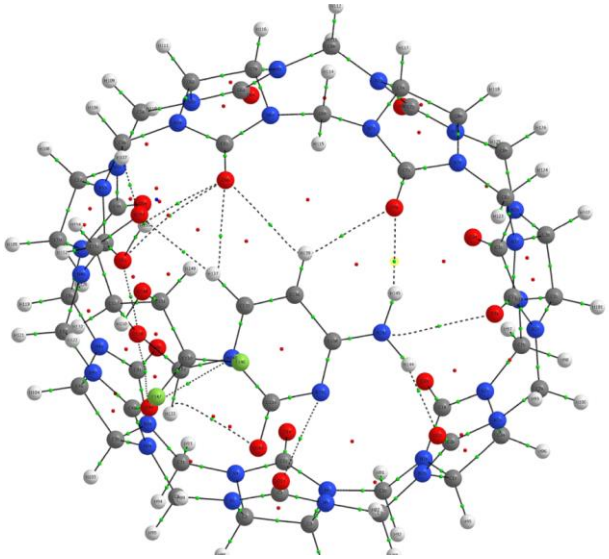

Figure 6. Same as Figure 5 For CB[7]/Gem3.

4. CONCLUSIONS

Eight configurations of noncovalent interactions of cucurbit[7]uril (CB[7]) with drug gemcitabine (Gem) were studied at M06-2X density functional level in the gas phase as well as the aqueous solution. According to the binding energies, the adsorption of Gem on the internal and external surface of CB[7] is favorable and all host-guest complexes are stable. The configuration related to the internal surface adsorption is the most stable configuration. The values of solvation energies related to all configurations are more negative than those of Gem, showing the drug solubility increases in the presence of CB[7]. Quantum molecular descriptors indicated that the drug reactivity increases in the vicinity of CB[7]. In addition, AIM analysis showed that Gem could be adsorbed on CB[7] surface through hydrogen bonds between drug and carrier. The AIM results confirmed that the highest number of hydrogen bonds exist in the most stable configuration (CB[7]/Gem1).

5. REFERENCES

[1] Li X., *Design of controlled release drug delivery systems*, McGraw Hill Professional, **2005.**

[2] Vivero-Escoto J.L., Slowing I.I., Trewyn B.G., Lin V.S.Y., Mesoporous silica nanoparticles for intracellular controlled drug delivery, *Small*, 6, 18, 1952-67, **2010.**

[3] Iurie R., Cell drug delivery of fluorescein loaded ApoB100 functionalized liposomes, *Biointerface Research in Applied Chemistry*, 5, 6, 1007-1010, **2015.**

[4] Krause-Heuer A.M., Grant M.P., Orkey N., Aldrich-Wright J.R., Drug delivery devices and targeting agents for platinum (II) anticancer complexes, *Australian Journal of Chemistry*, 61, 9, 675-81, **2008.**

[5] Kemp S., Wheate N.J., Wang S., Collins J.G., Ralph S.F., et al, Encapsulation of platinum (II)-based DNA intercalators within cucurbit [6, 7, 8] urils, *JBIC Journal of Biological Inorganic Chemistry*, 12, 7, 969-79, **2007.**

[6] Jiang G., Li G., Preparation and biological activity of novel cucurbit [8] uril–fullerene complex, *Journal of Photochemistry and Photobiology B: Biology*, 85, 3, 223-7, **2006.**

[7] Grumezescu A.M., Andronescu E., Ficai A., Bleotu C., Chifiriuc M.C., Chitin based biomaterial for antimicrobial therapy: fabrication, characterization and in vitro profile based interaction with eukaryotic and prokaryotic cells, *Biointerface Research in Applied Chemistry*, 2, 5, 438-445, **2012.**

[8] Saleh N., Khaleel A., Al-Dmour H., al-Hindawi B., Yakushenko E., Host–guest complexes of cucurbit [7] uril with albendazole in solid state, *Journal of Thermal Analysis and Calorimetry*, 111, 1, 385-92, **2013.**

[9] Naik D.R., Raval J.P., Characteristic and controlled release of antiviral drug: A comparative study on preparative techniques and polymer affected parameter, *Biointerface Research in Applied Chemistry*, 2, 5, 409-416, **2012.**

[10] Ghosh I., Nau W.M., The strategic use of supramolecular pKa shifts to enhance the bioavailability of drugs, *Advanced drug delivery reviews*, 64, 9, 764-83, **2012.**

[11] Day A.I., Collins J.G., Cucurbituril receptors and drug delivery, *Supramolecular Chemistry: From Molecules to Nanomaterials*, **2012.**

[12] Saleh N., Al-Soud Y.A., Al-Kaabi L., Ghosh I., Nau W.M., A coumarin-based fluorescent PET sensor utilizing supramolecular pKa shifts, *Tetrahedron Letters*, 52, 41, 5249-54, **2011.**

[13] Saleh N., Al-Rawashdeh N.A., Fluorescence enhancement of carbendazim fungicide in cucurbit [6] uril, *Journal of fluorescence*, 16, 4, 487-93, **2006.**

[14] Bhasikuttan A.C., Mohanty J., Nau W.M., Pal H., Efficient Fluorescence Enhancement and Cooperative Binding of an Organic Dye in a Supra-biomolecular Host–Protein Assembly, *Angewandte Chemie*, 119, 22, 4198-200, **2007.**

[15] Liu H., Wu X., Huang Y., He J., Xue S.-F., et al, Improvement of antifungal activity of carboxin by inclusion complexation with cucurbit [8]uril, *Journal of Inclusion Phenomena and Macrocyclic Chemistry*, 71, 3-4, 583-7, **2011.**

[16] Barooah N., Mohanty J., Pal H., Bhasikuttan A.C., Supramolecular assembly of hoechst-33258 with cucurbit[7]uril macrocycle, *Physical Chemistry Chemical Physics*, 13, 28, 13117-26, **2011.**

[17] Freeman W., Mock W., Shih N., Cucurbituril, *Journal of the American Chemical Society*, 103, 24, 7367-8, **1981.**

[18] Lo S.-C., Burn P.L., Development of dendrimers: macromolecules for use in organic light-emitting diodes and solar cells, *Chemical Reviews*, 107, 4, 1097-116, **2007.**

[19] Caminade A.M., Maraval A., Majoral J.P., Phosphorus-Containing Dendrons: Synthesis, Reactivity, Properties, and Use as Building Blocks for Various Dendritic Architectures, *European Journal of Inorganic Chemistry*, 2006, 5, 887-901, **2006.**

[20] Connors K.A., The stability of cyclodextrin complexes in solution, *Chemical Reviews*, 97, 5, 1325-58, **1997.**

[21] Kim J., Jung I.-S., Kim S.-Y., Lee E., Kang J.-K., et al, New cucurbituril homologues: syntheses, isolation, characterization, and X-ray crystal structures of cucurbit [n] uril (n= 5, 7, and 8), *Journal of the American Chemical Society*, 122, 3, 540-1, **2000.**

[22] Liu S., Zavalij P.Y., Isaacs L., Cucurbit[10]uril, *Journal of the American Chemical Society*, 127, 48, 16798-9, **2005.**

[23] Wheate N.J., Cucurbit[n]uril: A new molecule in host-guest chemistry, *Australian Journal of Chemistry*, **2006.**

[24] Jeon W.S., Moon K., Park S.H., Chun H., Ko Y.H., et al, Complexation of ferrocene derivatives by the cucurbit[7]uril host: a comparative study of the cucurbituril and cyclodextrin host families, *Journal of the American Chemical Society*, 127, 37, 12984-9, **2005.**

[25] Walker S., Oun R., McInnes F.J., Wheate N.J., The potential of cucurbit[n]urils in drug delivery, *Israel Journal of Chemistry*, 51, 5-6, 616-24, **2011.**

[26] Lagona J., Mukhopadhyay P., Chakrabarti S., Isaacs L., The cucurbit [n]uril family, *Angewandte Chemie International Edition*, 44, 31, 4844-70, **2005.**

[27] Mock W.L., Shih N.Y., Structure and selectivity in host-guest complexes of cucurbituril, *The Journal of organic chemistry*, 51, 23, 4440-6, **1986.**

[28] Ol'ga A., Samsonenko D.G., Fedin V.P., Supramolecular chemistry of cucurbiturils, *Russian Chemical Reviews*, 71, 9, 741-60, **2002**.

[29] Buck D.P., Abeysinghe P.M., Cullinane C., Day A.I., Collins J.G., Harding M.M., Inclusion complexes of the antitumour metallocenes Cp2MCl2 (M= Mo, Ti) with cucurbit[n]urils, *Dalton Transactions*, 17, 2328-34, **2008.**

[30] Lagona J., Wagner B.D., Isaacs L., Molecular-recognition properties of a water-soluble cucurbit[6]uril analogue, *The Journal of organic chemistry*, 71, 3, 1181-90, **2006.**

[31] Wang R., Macartney D.H., Cucurbit[7]uril host–guest complexes of the histamine H2-receptor antagonist ranitidine, *Organic & biomolecular chemistry*, 6, 11, 1955-60, **2008.**

[32] Rankin M.A., Wagner B.D., Fluorescence enhancement of curcumin upon inclusion into cucurbituril, *Supramolecular Chemistry*, 16, 7, 513-9, **2004.**

[33] Kemp S., Wheate N.J., Stootman F.H., Aldrich-Wright J.R., The host-guest chemistry of Proflavine with cucurbit[6, 7, 8]urils, *Supramolecular Chemistry*, 19, 7, 475-84, **2007.**

[34] Wheate N.J., Improving platinum (II)-based anticancer drug delivery using cucurbit[n]urils, *Journal of Inorganic Biochemistry*, 102, 12, 2060-6, **2008.**

[35] Jeon Y.J., Kim S.-Y., Ko Y.H., Sakamoto S., Yamaguchi K., Kim K., Novel molecular drug carrier: encapsulation of oxaliplatin in cucurbit[7]uril and its effects on stability and reactivity of the drug, *Organic & biomolecular chemistry*, 3, 11, 2122-5, **2005.**

[36] Shchepotina E., Pashkina E., Yakushenko E., Kozlov V., Cucurbiturils as containers for medicinal compounds, *Nanotechnologies in Russia*, 6, 11-12, 773-9, **2011.**

[37] Halterman R.L., Moore J.L., Yakshe K.A., Halterman J.A., Woodson K.A., Inclusion complexes of cationic xanthene dyes in cucurbit[7]uril, *Journal of Inclusion Phenomena and Macrocyclic Chemistry*, 66, 3-4, 231-41, **2010.**

[38] Arunkumar E., Forbes C.C., Smith B.D., Improving the properties of organic dyes by molecular encapsulation, *European Journal of Organic Chemistry*, 2005, 19, 4051-9, **2005.**

[39] Montes-Navajas P., Corma A., Garcia H., Complexation and fluorescence of tricyclic basic dyes encapsulated in cucurbiturils, *ChemPhysChem*, 9, 5, 713-20, **2008.**

[40] Mohanty J., Nau W.M., Ultrastable rhodamine with cucurbituril, *Angewandte Chemie*, 117, 24, 3816-20, **2005.**

[41] Mohanty J., Pal H., Ray A.K., Kumar S., Nau W.M., Supramolecular dye laser with cucurbit[7]uril in water, *ChemPhysChem*, 8, 1, 54-6, **2007.**

[42] Hettiarachchi G., Nguyen D., Wu J., Lucas D., Ma D., et al, Toxicology and drug delivery by cucurbit[n]uril type molecular containers, *PLoS ONE*, 5, 5, e10514, **2010.**

[43] Nau W.M., Supramolecular capsules: under control, *Nature chemistry*, 2, 4, 248, **2010.**

[44] Uzunova V.D., Cullinane C., Brix K., Nau W.M., Day A.I., Toxicity of cucurbit[7]uril and cucurbit [8] uril: an exploratory in vitro and in vivo study, *Organic & biomolecular chemistry*, 8, 9, 2037-42, **2010.**

[45] Teymoori M., Morsali A., Bozorgmehr M., Beyramabadi S., Comprehensive quantum mechanical study on th mechanistic, energetic and structural properties of adsorption of drug 6-thioguanine onto functionalized carbon nanotubes, *Digest Journal of Nanomaterials & Biostructures (DJNB)*, 12, 3, **2017.**

[46] Chegini H., Morsali A., Bozorgmehr M., Beyramabadi S., Theoretical study on the mechanism of covalent bonding of dapsone onto functionalised carbon nanotubes: effects of coupling agent, *Progress in Reaction Kinetics and Mechanism*, 41, 4, 345-55, **2016.**

[47] Khorram R., Morsali A., Raissi H., Hakimi M., BEYRAMABADI S A., Mechanistic, Energetic and Structural Aspects of the Adsorption of Carmustine on the Functionalized Carbon Nanotubes, *Chinese Journal of Structural Chemistry*, 10, 007, **2017.**

[48] Osikoya A., Wankasi D., Vala R., Afolabi A., Dikio E., Synthesis, Characterization and adsorption studies of fluorine–doped carbon nanotubes, *Digest Journal of Nanomaterials and Biostructures*, 9, 3, 1187-97, **2014.**

[49] Salehi R., Rasoolzadeh R., Investigation of Capecitabine and 5-fluorouracil anticancer drugs structural properties and their interactions

with single-walled carbon nanotube: insights from computational methods, *Biointerface Research in Applied Chemistry*, 8, 1, 3075-83, **2018.**
[50] Kamel M., Raissi H., Morsali A., Shahabi M., Assessment of the adsorption mechanism of Flutamide anticancer drug on the functionalized single-walled carbon nanotube surface as a drug delivery vehicle: An alternative theoretical approach based on DFT and MD, *Applied Surface Science*, 434, 492-503, **2018.**
[51] Zheng Y.B., Kiraly B., Huang T.J., Molecular machines drive smart drug delivery, *Nanomedicine*, 5, 9, 1309-12, **2010.**
[52] Linko V., Ora A., Kostiainen M.A., DNA nanostructures as smart drug-delivery vehicles and molecular devices, *Trends in Biotechnology*, 33, 10, 586-94, **2015.**
[53] Szymański W., Beierle J.M., Kistemaker H.A., Velema W.A., Feringa B.L., Reversible photocontrol of biological systems by the incorporation of molecular photoswitches, *Chemical Reviews*, 113, 8, 6114-78, **2013.**
[54] Denny W.A., Prospects for hypoxia-activated anticancer drugs, *Current Medicinal Chemistry-Anti-Cancer Agents*, 4, 5, 395-9, **2004.**
[55] Zeman E.M., Brown J.M., Lemmon M.J., Hirst V.K., Lee W.W., SR-4233: a new bioreductive agent with high selective toxicity for hypoxic mammalian cells, *International Journal of Radiation Oncology* Biology* Physics*, 12, 7, 1239-42, **1986.**
[56] Frisch M., Trucks G., Schlegel H., Scuseria G., Robb M., et al, G09 Gaussian Inc, *Wallingford, CT*, **2009.**
[57] Morsali A., Hoseinzade F., Akbari A., Beyramabadi S.A., Ghiasi R., Theoretical Study of Solvent Effects on the Cis-to-Trans Isomerization of [Pd (C6Cl2F3) I (PH3) 2], *Journal of Solution Chemistry*, 42, 10, 1902-11, **2013.**
[58] Beyramabadi S.A., Eshtiagh-Hosseini H., Housaindokht M.R., Morsali A., Mechanism and kinetics of the Wacker process: a quantum mechanical approach, *Organometallics*, 27, 1, 72-9, **2007.**
[59] Gharib A., Morsali A., Beyramabadi S., Chegini H., Ardabili M.N., Quantum mechanical study on the rate determining steps of the reaction between 2-aminopyrimidine with dichloro-[1-methyl-2-(naphthylazo) imidazole] palladium (II) complex, *Progress in Reaction Kinetics and Mechanism*, 39, 4, 354-64, **2014.**
[60] Morsali A., Mechanism of the Formation of Palladium (II) Maleate Complex: A DFT Approach, *International Journal of Chemical Kinetics*, 47, 2, 73-81, **2015.**
[61] Ardabili M.N., Morsali A., Beyramabadi S.A., Chegini H., Gharib A., Quantum mechanical study of the alkoxide-independent pathway of reductive elimination of C–O from palladium (p-cyanophenyl) neopentoxide complex, *Research on Chemical Intermediates*, 41, 8, 5389-98, **2015.**
[62] Cammi R., Tomasi J., Remarks on the use of the apparent surface charges (ASC) methods in solvation problems: Iterative versus matrix-inversion procedures and the renormalization of the apparent charges, *Journal of Computational Chemistry*, 16, 12, 1449-58, **1995.**
[63] Tomasi J., Persico M., Molecular interactions in solution: an overview of methods based on continuous distributions of the solvent, *Chemical Reviews*, 94, 7, 2027-94, **1994.**
[64] Marenich A.V., Cramer C.J., Truhlar D.G., Universal solvation model based on solute electron density and on a continuum model of the solvent defined by the bulk dielectric constant and atomic surface tensions, *Journal of Physical Chemistry B*, 113, 18, 6378-96, **2009.**
[65] Keith T.A., AIMAll (Version 13.05. 06), *TK Gristmill Software, Overland Park KS, USA*, **2013.**
[66] Bader R.F., A quantum theory of molecular structure and its applications, *Chemical Reviews*, 91, 5, 893-928, **1991.**
[67] Bader R.F., *Atoms in molecules*, Wiley Online Library, **1990.**
[68] Parr R.G., Szentpaly L.v., Liu S., Electrophilicity index, *Journal of the American Chemical Society*, 121, 9, 1922-4, **1999.**
[69] Rozas I., Alkorta I., Elguero J., Behavior of ylides containing N, O, and C atoms as hydrogen bond acceptors, *Journal of the American Chemical Society*, 122, 45, 11154-61, **2000.**
[70] Espinosa E., Souhassou M., Lachekar H., Lecomte C., Topological analysis of the electron density in hydrogen bonds, *Acta Crystallographica Section B: Structural Science*, 55, 4, 563-72, **1999.**